

Influence of parametric forcing on the nonequilibrium dynamics of wave patterns

S. I. Abarzhi, O. Desjardins, A. Nepomnyashchy, and H. Pitsch

Department of Applied Mathematics, Illinois Institute of Technology, Chicago, Illinois 60616, USA;

FLASH Center, The University of Chicago, Chicago, Illinois 60637, USA;

Department of Mathematics and Minerva Center for Nonlinear Physics of Complex Systems,

Technion–Israel Institute of Technology, Haifa 32000, Israel;

and Center for Turbulence Research, Stanford University, Stanford, California 94305, USA

(Received 19 May 2006; revised manuscript received 1 December 2006; published 12 April 2007)

We investigate analytically and numerically the effect of inhomogeneities on the nonequilibrium dynamics of wave patterns in the framework of a complex Ginzburg-Landau equation (CGLE) with parametric, nonresonant forcing periodic in space and time. It is found that the forcing results in occurrence of traveling waves with different dispersion properties. In the limiting case of forcing with very large wavelength, the waves have essentially anharmonic spatial structure. We consider the influence of modulations on the development of an intermittent chaos and show that the parametric forcing may completely suppress the appearance of chaotic patterns. The relations between this and other pattern-forming systems are discussed. The results obtained are applied to describe the dynamics of thermal Rossby waves influenced by surface topography.

DOI: 10.1103/PhysRevE.75.046208

PACS number(s): 89.75.Kd, 47.54.-r, 47.52.+j, 05.45.Pq

I. INTRODUCTION

Pattern formation occurs in a wide variety of natural nonequilibrium systems and displays many common features of the dynamics [1]. This universality is well captured by the low-dimensional theoretical models and by the laboratory experiments [1,2]. The models and the experiments focus on studies of nonequilibrium phenomena and transitions to deterministic chaos in ideal, spatially extended homogeneous systems [1,2]. Many natural systems are however inhomogeneous. The heterogeneities induce spatial and temporal modulations, which affect significantly the pattern formation, and this influence is far from being completely understood [1,2]. Here we consider the effect of modulations on the nonequilibrium dynamics of wave patterns, and report analytical and numerical solutions for the complex Ginzburg-Landau equation (CGLE) with parametric forcing periodic in space and time.

The complex Ginzburg-Landau equation

$$\frac{\partial A}{\partial T} = \beta \frac{\partial^2 A}{\partial Y^2} + \Delta_0 A + D|A|^2 A \quad (1)$$

is one of the generic models for studies of nonequilibrium dynamics of spatially extended homogeneous systems, including spontaneous wave modulation, spatiotemporal chaos, intermittency, and oscillatory long-wave instability [2,3]. In Eq. (1), Y and T are the slow space and time variables, and $A(Y, T)$ is a complex envelope function (e.g., the “amplitude function”) of a slowly modulated short-wave system in the frame of reference moving with the wave group velocity [4,5]. The growth-rate coefficient Δ_0 in Eq. (1) is real and positive. The coefficients β and D are complex, $\beta = \beta_r + i\beta_i$, $D = D_r + iD_i$, where the subscripts r and i mark the real and imaginary parts, and $\beta_r > 0$ and $D_r < 0$ according to the stability criterion [2,6]. Equation (1) balances the processes of the linear growth of the amplitude near the instability threshold and its nonlinear saturation, augmented with diffusion, dispersion, and the nonlinear frequency shift. The model (1)

describes the dynamics of a system invariant under the spatiotemporal translations and gauge transformation $A \rightarrow A \exp(i\phi)$, $\phi = \text{const}$. The former symmetry is related to translations of the large-scale wave envelope, whereas the latter symmetry manifests the invariance to spatiotemporal translations of the underlying short-scale wave patterns. The interaction between large and small scales is a nonadiabatic effect, and it is neglected in the framework of the CGLE [7]. The heuristic equation (1) can be rigorously derived from the first principles for a variety of physical systems, such as optical systems, Faraday ripples, and rotating fluids [4,8]. Numerous studies of the CGLE dynamics are summarized in the review article by Aranson and Kramer [2].

Our understanding of order and chaos has been significantly advanced by the concept of universality [1,2], yet, the problem still sustains the efforts applied. An important issue is a qualitative and quantitative correspondence between the idealized, low-dimensional model description and a real, heterogeneous and multiscale phenomenon. The problem can be viewed on one hand as a sensitivity of the model results to heterogeneities and noise, which are always present and often hard to grip on in observations, and on the other hand—as a control of the diverse pattern formation phenomena by means of heterogeneities.

First attempts to study the effect of heterogeneities on the nonlinear pattern-forming system have been made in the 1970s and 1980s [9,10]. The nonequilibrium dynamics of steady patterns influenced by a slowly relaxed Goldstone mode or forced stochastically with time have been considered in Refs. [11–14]. The representative laboratory experiments are, respectively, surface-tension-driven convection [15] and the electrically driven convection in nematic crystals [16]. In these cases, a real Ginzburg-Landau equation is augmented with a forcing term (e.g., the additive noise), which represents the modulations of the control parameter and results in the essentially nonlocal character of the pattern stability [11–14].

For the complex Ginzburg-Landau equation, the case of a resonant spatially periodic short-wave perturbation has been

considered, with the perturbation wavelength close to or multiple of the characteristic wavelength of the pattern. This kind of perturbations augments the CGLE with an additional term, which violates the gauge symmetry, while the invariance of the envelope function to translations is kept. A generalization of this theory to the case of an oscillatory instability has been considered in Refs. [17,18]. Similar modification of the amplitude equation is produced by a resonant time-periodic forcing [19].

The violation of the gauge symmetry of the CGLE by parametric forcing has been a subject of numerous studies. The analysis of synchronization, modulation, and depinning phenomena [20–22], creation of two-dimensional patterns [23], and dynamics of patterns and fronts for higher resonances ([24–27], and references therein) are to mention a few. In the present paper, we consider another type of forcing, that is the long-wave modulation of the system's parameters whose characteristic spatial and temporal scales are comparable with the characteristic scales of the complex Ginzburg-Landau equation. This type of forcing does not violate the gauge theory and induces a dependence of the coefficients in the amplitude equation (1) on slow variables Y and T . As in the region of validity of CGLE, the linear growth is small, then, to the leading order, only the growth rate coefficient Δ_0 in Eq. (1) should be modified by the modulations.

The studies of the CGLE with nonconstant coefficients are still rather rare. Some special cases have been analyzed by Malomed in the context of binary-fluid convection in a narrow channel. In [28], he has considered a parameter ramp, which matches smoothly the subcritical and supercritical regions of the channel, and has studied the ramp-induced mechanism of the wave vector selection. Reference [29] analyzes the destabilization of the traveling waves and trapping a solitary pulse by a smooth inhomogeneity. Zimmermann *et al.* [30] considered a Swift-Hohenberg equations with the stochastic modulation of the linear growth rate and an inhomogeneous stochastic term. An interesting problem of the interaction of traveling waves with a spatially modulated coefficient of the nonlinear interaction has been discussed in Ref. [31]. A modification of the CGLE, which contains an additional non-gauge-invariant term γA^* corresponding to a subharmonic resonant forcing, has been considered in the case of a spatially dependent coefficient γ in [32]. Very recently, the CGLE with a spatially modulated growth rate has been applied for the analysis of the competition between harmonic and subharmonic oscillations in a spatially forced oscillating chemical reaction [33]. However, to the best of the authors' knowledge, general case of the influence of periodic (in space and time) nonresonant parametric forcing on the nonequilibrium dynamics of wave patterns governed by CGLE has never been investigated.

As a representative example of such inhomogeneous system, one may consider, for instance, laser pulse propagation in optical fibers and a magnetoconvection of rotating fluids driven by a modulated magnetic field, or as an effect of the surface topography on the dynamics of the Rossby waves in geophysics. It is generally accepted that thermal Rossby waves transport the angular momentum and internal heat in the liquid outer core of the Earth [8]. These transports are

influenced significantly by the surface topography, i.e., by the heterogeneities of the mantle-core boundary [34,35]. In the laboratory, thermal Rossby waves have been studied in experiments in a rotating liquid-filled sphere and in a cylindrical annulus [36]. To model the effect of surface topography, the authors of Refs. [37–39] have considered the dynamics of thermal Rossby waves in a cylindrical annulus with azimuthally modulated height, and have found in several special cases the analytical and numerical solutions for the system of the Navier-Stokes equations. The solutions obtained have been interpreted as modulated Rossby waves and as traveling waves [37–39]. Still a need remains in a model, which could describe the effect of modulations on the dynamics of Rossby waves in a wide range of the forcing parameters and convection intensity, and could link this inhomogeneous system to other pattern-forming systems.

The present work considers the influence of periodic nonresonant parametric forcing on the nonequilibrium dynamics of wave patterns governed by the complex Ginzburg-Landau equation. We find analytical and numerical solutions for the modulated CGLE and show that the forcing causes the appearance of traveling waves with different dispersion properties. If the forcing wavelength is very large, the waves have essentially anharmonic spatial structure. The effect of modulations on the development of an intermittent chaos is considered. The results obtained indicate that the forcing can regularize chaotic patterns and completely suppress the development of the intermittent chaos [40]. We discuss the relations of this pattern-forming system to other ones and apply the results obtained to describe the effect of surface topography on the dynamics of thermal Rossby waves [8,38,39].

II. DYNAMICAL SYSTEM

The Boussinesq convection in a rotating cylindrical annulus with homogeneous boundaries is characterized by the convective rolls, which move in the azimuthal direction and oscillate in space and time [8]. These are the thermal Rossby waves. Their nonlinear dynamics and pattern formation are governed by the complex Ginzburg-Landau equation, which can be derived from the system of the Navier-Stokes equations near the convection onset [42]. If the annulus boundaries are modulated, the convection process is multiscale and heterogeneous. For heterogeneous systems a rigorous derivation of the amplitude equation from the conservation laws is an unresolved problem [1,2]. As discussed in the foregoing, to model the nonlinear dynamics of a slightly inhomogeneous system, we augment the complex Ginzburg-Landau equation (1) with the parametric forcing term:

$$\frac{\partial A}{\partial T} = \beta \frac{\partial^2 A}{\partial Y^2} + \Delta_0 A + D|A|^2 A + f(Y - VT)A. \quad (2)$$

Equation (2) is written in the frame of reference moving with the group velocity V of the waves. Without forcing, $f=0$, the problem is homogeneous, and the values of Δ_0 , $D_{i(r)}$, and $\beta_{i(r)}$ are determined by the parameters of the convective process [42]. If $D_i/|D_r| < 1$ and $\beta_i/\beta_r < 1/2$, the convective patterns with $A = \bar{A}$ appear for $\Delta_0 > \beta_r q^2$,

$$\bar{A} = A_0 e^{iqY + i\gamma_0 T}, \quad A_0^2 = -\frac{(\Delta_0 - \beta_r q^2)}{D_r}, \quad \gamma_0 = -\beta_i q^2 + D_i A_0^2. \quad (3)$$

The primary solution, Eq. (3), describes the pattern with a wave vector close to the characteristic wave vector of the convection onset. This solution is stable if $\Delta_0 - \beta_r q^2 > 0$. If $\beta_i/\beta_r \geq 1/2$ and $D_i \beta_i/|D_r| \beta_r > 1$, the homogeneous system evolves to spatiotemporal chaos through intermittency [40,41].

In general case, the parametric forcing in Eq. (2) is complex and influences both the growth-rate and the linear frequency of the wave patterns. In geophysical applications, the dependence of the linear frequency on the forcing can be neglected [8] and we consider

$$f(Y - VT) = \delta e^{ik(Y-VT)} + \delta^* e^{-ik(Y-VT)}, \quad (4)$$

where δ and k are the forcing amplitude and wave vector with $|\delta|k \ll 1$, and the star marks the complex conjugate. We find analytical and numerical solutions for system (2) and (4) and investigate the effect of the modulations on the formation of nonchaotic and chaotic wave patterns.

III. ANALYTICAL SOLUTIONS

In this section we derive analytical solutions for the heterogeneous system (2) and (4) and describe the asymptotic dynamics of nonchaotic wave patterns.

A. Regular asymptotic dynamics

When the values of $\beta_i/\beta_r \leq 1/2$ and $D_i \beta_i/|D_r| \beta_r < 1$, the homogeneous system exhibits nonchaotic dynamics [40], and the parametric forcing (4) transforms the primary solution (3) into a modulated quasiperiodic wave,

$$A(Y, T) = e^{iqY + i\gamma T} a(Y - VT, T). \quad (5)$$

Here $a(Y - VT, T)$ is a complex envelope function of the variables $(Y - VT)$ and T , and in the general case $\gamma \neq \gamma_0$. In the regular case, the amplitude a in Eq. (5) can be presented in the form

$$a(Y - VT, T) = a_0(T) + \sum_{n=1}^{\infty} [a_n(T) e^{-ink(Y-VT)} + b_n(T) e^{ink(Y-VT)}], \quad (6)$$

where $a_n(T)$, $b_n(T)$, and $a_0(T)$ are time-dependent Fourier amplitudes, and, without loss of generality, the value of a_0 is real, Eq. (3).

Substituting Eq. (6) in Eqs. (2) and (4), we eliminate the explicit dependence on the coordinate and time and derive an infinite system of coupled equations for the Fourier amplitudes:

$$\frac{\partial a_0}{\partial T} = [f_0 + Da_0^2 + 2D(a_1 a_1^* + b_1 b_1^* + a_1 b_1)] a_0 + \dots, \quad (7)$$

$$\begin{aligned} \frac{\partial a_1}{\partial T} = & f_1^- a_1 + db_1^* + [D(a_1 a_1^* + 2b_1 b_1^*) a_1 \\ & + 2Da_0(a_1^* a_2 + a_2 b_1 + b_1 b_2^*)] + a_0 \delta + \dots, \end{aligned} \quad (8)$$

$$\begin{aligned} \frac{\partial b_1}{\partial T} = & da_1^* + f_1^+ b_1 + [D(2a_1 a_1^* + b_1 b_1^*) b_1 \\ & + 2Da_0(a_1 a_2^* + a_1 b_2 + b_1^* b_2)] + a_0 \delta^* + \dots, \end{aligned} \quad (9)$$

$$\frac{\partial a_2}{\partial T} = f_2^- a_2 + db_2^* + [Da_0(2a_1 b_1^* + a_1^2)] + a_1 \delta + \dots, \quad (10)$$

$$\begin{aligned} \frac{\partial b_2}{\partial T} = & da_2^* + f_2^+ b_2 + [Da_0(2a_1^* b_1 + b_1^2)] + b_1 \delta^* + \dots, \end{aligned} \quad (11)$$

where $f_0 = \Delta_0 - \beta q^2 - i\gamma$, $f_n^\pm = \Delta_0 - \beta(q \pm nk)^2 - i(\gamma \mp nkV) + 2d$ with $n=1, 2, \dots$ and $d = Da_0^2$. The dynamics of system (7)–(11) depends on the control parameter Δ_0 , the wave vector q , and the forcing parameters δ and k .

For the sake of simplicity, we focus below on the case of zero group velocity, i.e., $V=0$. If the value of Δ_0 is finite, the wavelength of the modulation $1/k$ is finite and the amplitude δ is small, then, in zero order in δ/Δ_0 the solution for system (7)–(11) coincides with the primary homogeneous solution, i.e., $a_0 = A_0$, $\gamma = \gamma_0$, and $a_n = b_n = 0$ for $n=1, 2, \dots$ (3). In linear in δ/Δ_0 approximation, the system (7)–(11) is reduced to

$$\frac{\partial a_1}{\partial T} = f_1^- a_1 + db_1^* + a_0 \delta, \quad \frac{\partial b_1}{\partial T} = d^* a_1 + (f_1^+)^* b_1^* + a_0 \delta. \quad (12)$$

Equations (12) have solutions with steady $a_1 = A_1$ and $b_1 = B_1$, where

$$A_1 = -\frac{a_0 \delta [(f_1^+)^* - d]}{[f_1^- (f_1^+)^* - dd^*]}, \quad B_1^* = -\frac{a_0 \delta (f_1^- - d^*)}{[f_1^- (f_1^+)^* - dd^*]}. \quad (13)$$

In the framework of system (12), the modulated solution $A = e^{iqY + i\gamma_0 T} (A_0 + A_1 e^{-ikY} + B_1 e^{ikY})$ is stable, if the growth rate σ of a slightly perturbed solution satisfies the condition $\text{Re}[\sigma] < 0$, where σ obeys the equation

$$(\sigma + 2f_0) \{ (\sigma - f_1^-) [\sigma - (f_1^+)^*] - dd^* \} = 0. \quad (14)$$

The region of stability of the modulated solution $A = e^{iqY + i\gamma_0 T} (A_0 + A_1 e^{-ikY} + B_1 e^{ikY})$ is narrower compared to that of the primary solution (3).

For nonlinear solutions for systems (2)–(4) and (7)–(11), the value of a_0 deviates from A_0 , higher order terms with wave vectors $(q \pm nk)$ appear in the expansion (6), and the time dependence and the region of the Eckhaus stability change. The linear solutions (12) and (13) indicate that the system (2) and (4) may have a nontrivial nonequilibrium dynamics if the wavelength of the modulation is very large. Indeed, as k decreases, the amplitudes A_1 , B_1 in Eq. (13), and therefore a_n and b_n in Eqs. (7)–(11) increase and approach the same or higher order of magnitude than a_0 . In this case, the harmonic expansion (6)–(11) may not be applicable, and

the nonlinear dynamics in system (2) and (4) can be described via a long-wave expansion.

B. Anharmonic asymptotic solutions for large-scale modulations

To find the nonlinear solutions in the case of modulations with very large wavelength, we reduce the Ginzburg-Landau equation [(2) and (4)] to a standard form,

$$A_T = (1 + \tilde{f})A + (1 + ic_1)A_{YY} - (1 - ic_2)|A|^2A, \quad (15)$$

where the subscript denotes the differentiation with respect to the corresponding variable. We assume that \tilde{f} does not depend on time T and it is a 2π periodic function of the coordinate kY , i.e., $\tilde{f} = \tilde{f}(kY)$, and $0 < k \ll 1$. Then, with $A = R(Y, T)\exp(i\Theta(Y, T))$, Eq. (15) is transformed into the system

$$R_T = [1 + \tilde{f} - \Theta_Y^2 - R^2]R - c_1(2R_Y\Theta_Y + R\Theta_{YY}) + R_{YY}, \quad (16)$$

$$R\Theta_T = 2R_Y\Theta_Y + R\Theta_{YY} + c_1(R_{YY} - R\Theta_Y^2) + c_2R^3. \quad (17)$$

Without forcing, $\tilde{f} = 0$ in Eq. (15), the group velocity of a disturbance propagating on the background of a periodic wave is proportional to $(c_1 + c_2)$ [2]. The solution for the system (16) and (17) depends therefore on the value of $(c_1 + c_2)$.

In the *nonresonant case* with $c_1 + c_2 \neq 0$, we define the slow variable $y = kY$, represent the solution in the form of a spatially modulated and temporally monochromatic wave with $R = R(y)$, $\Theta = \theta(Y) + i\gamma T$, $\theta_Y = Q(y)$, and expand the amplitude $R = R_0(y) + kR_1(y) + \dots$ and the wave vector $Q = Q_0(y) + kQ_1(y) + \dots$ in terms of small k . Substituting these dependencies in Eqs. (16) and (17), we find to the leading order

$$Q_0^2 = -\frac{\gamma - c_2(1 + \tilde{f})}{c_1 + c_2}, \quad R_0^2 = \frac{\gamma + c_1(1 + \tilde{f})}{c_1 + c_2}. \quad (18)$$

We see that the modulations of the local wave vector and the local amplitude are in phase when the coefficients c_1 and c_2 have the same sign, and are out of phase when c_1 and c_2 have the opposite signs. Solution (18) is valid, if $Q_0^2(y) > 0$ and $R_0^2(y) > 0$ and γ obeys the relation $\gamma_{max} > \gamma > \gamma_{min}$, where $\gamma_{max} = \min(c_2(1 + \tilde{f}))$ and $\gamma_{min} = \max(-c_1(1 + \tilde{f}))$ for $c_1 + c_2 > 0$. The condition of compatibility $\gamma_{max} > \gamma_{min}$ imposes certain limitations on the values of \tilde{f} . We see, therefore, that for a harmonic modulation with $\tilde{f} = 2\delta \cos y$ the nonlinear solution

$$A(Y, T) \sim R_0(kY)\exp\left[i\int_0^Y Q_0(kZ)dZ + i\gamma T\right] \quad (19)$$

is essentially anharmonic. Similarly, one can calculate the higher order corrections.

In the *resonant case* with $c_1 + c_2 = 0$, the group velocity in Eq. (15) is zero, and the effect of the forcing is especially

TABLE I. Parameter values for nonchaotic runs.

Run	$(qL)/(2\pi)$	δ	$(kL)/(2\pi)$	V
A0	10	0	0	0
A1	10	0.1+0.1i	2	0
A2	10	0.2+0.2i	2	0
B1	2	0.1+0.1i	10	0
B2	2	0.2+0.2i	10	0
C1	10	0.1+0.1i	2	0.01
C2	10	0.2+0.2i	2	0.01
D1	2	0.1+0.1i	10	0.01
D2	2	0.2+0.2i	10	0.01

strong. In this case, the change of the sign of Q_0 leads to the appearance of sources and sinks of waves, while vanishing R_0 corresponds to the creation of a “black hole,” in agreement with the numerical solution discussed below in Sec. IV. A nonsingular, temporally monochromatic solution in the resonant case can be found for a relatively weak modulation with $\tilde{f} = kg$. Expanding $\gamma = \gamma_0 + \gamma_1 k + \dots$ in terms of small k , we obtain to the leading order that the amplitude R_0 is set by the local wave vector Q_0 ,

$$R_0^2 = 1 - Q_0^2, \quad \gamma_0 = -c_1, \quad (20)$$

which obeys the nonlinear equation $(1 + c_1^2)\frac{1 - 3Q_0^2}{1 - Q_0^2}Q_{0y} = c_1g(ky) + \gamma_1$. We integrate this equation and find for $Q_0(y)$ an implicit form

$$H(Q_0(y)) = H(Q_0(0)) + \frac{c_1}{1 + c_1^2} \int_0^y [g(kz) - \langle g \rangle] dz, \quad (21)$$

where $H(Q_0) \equiv 3Q_0 - \frac{1}{2} \ln \frac{1 + Q_0}{1 - Q_0}$ and $\langle g \rangle$ is the spatial average of g . If the wave vector Q_0 is in the region of the Eckhaus stability, $Q_0^2 < 1/3$, and the value of $H(Q_0(y))$ in Eq. (21) belongs to the interval $(-H_m, H_m)$, with $H_m = H(1/\sqrt{3})$, then the solution for Eq. (21) exists and is uniquely defined.

Based on the foregoing theoretical analysis, we conclude that for nonchaotic patterns governed by CGLE, the parametric forcing with a finite wavelength results in appearance of traveling waves, quasiperiodic in space and time (5). If the forcing wavelength is very large, the spatial structure of waves is essentially anharmonic, Eq. (19) and (20).

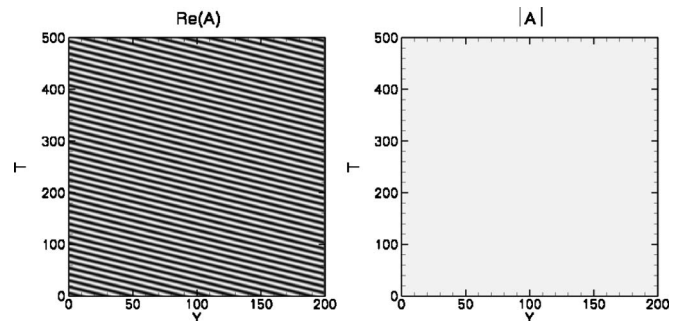


FIG. 1. Run A0, no forcing.

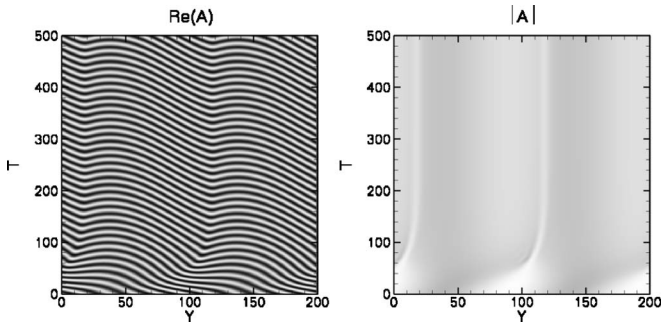


FIG. 2. Run A1, forcing with large wavelength, small amplitude, and zero group velocity.

IV. NUMERICAL SOLUTIONS

To describe the influence of parametric forcing on the formation of wave patterns and intermittent chaos, we find numerical solutions for the rescaled complex CGLE (15) in a wide range of the system parameters. In our simulations, the parametric forcing depends on the coordinate and time, $\tilde{f} = \tilde{\delta} e^{ik(Y-VT)} + \tilde{\delta}^* e^{ik(Y-VT)}$, and both chaotic and nonchaotic cases are considered, i.e., $(c_1, c_2) \in \mathbb{R}^2$:

$$A_T = A + (1 + ic_1)A_{YY} - (1 - ic_2)|A|^2 A + (\tilde{\delta} e^{i(kY-VT)} + \tilde{\delta}^* e^{i(kY-VT)})A. \quad (22)$$

The amplitude $A = A(Y, T)$ and initially $A(Y, T=0) = e^{iqY}$.

We solve Eq. (22) in the domain of size $L=200$ discretized on a mesh of 500 points. The spectral approach is used to compute the derivative of A with high accuracy. The boundary conditions in Y are periodic. Eq. (22) is integrated in time using a fully implicit solver. The solver is based on the backward differentiation formulas of the orders varied from 1 to 5 to adapt the stiffness of the problem. The integration time for all cases is 5000 time units, and the time step is automatically adjusted to enforce the integration accuracy. The real and imaginary parts, the magnitude and the phase of the amplitude A are calculated.

In the first series of runs we consider the influence of the parametric forcing on the formation of regular waves and choose the values of $c_1 \approx 0.2746$ and $c_2 \approx 0.6020$, which correspond to regular patterns in observations of [39]. The values of other parameters q , k , V , and $\tilde{\delta}$ are chosen to examine

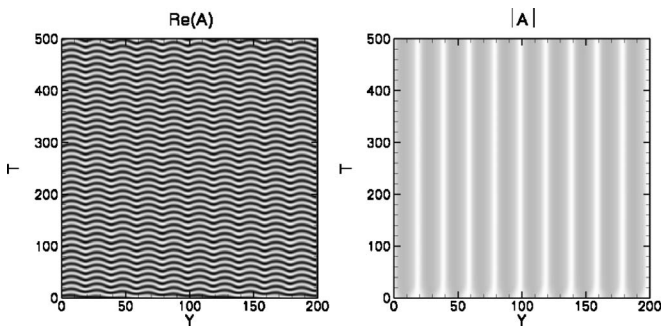


FIG. 3. Run B1, forcing with small wavelength, small amplitude, and zero group velocity.

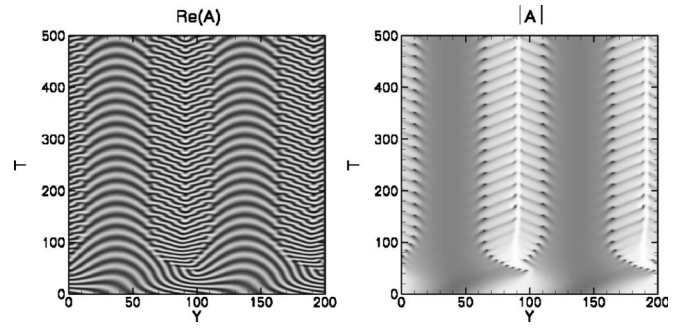


FIG. 4. Run A2, forcing with large wavelength, large amplitude, and zero group velocity.

the cases of forcing with large and small wavelengths, small and finite amplitude, with and without group velocity, see Table I.

The run A0 is the unforced reference case. The other runs employ the two different ratios of k/q and the forcing amplitude $\tilde{\delta}$, and account for the effect of the group velocity V . Figure 1 shows the contour plot of the real part $\text{Re}(A)$ and the magnitude $|A|$ of the amplitude A in the plane (Y, T) for the run A0 in Eq. (22), with darker regions marking higher values. The pattern represents a traveling wave, whose magnitude is independent of space and time. This numerical solution agrees quantitatively with the primary solution (3).

Figures 2 and 3 present numerical solutions for Eq. (22) for the run A1 with large forcing wavelength, $k/q=1/5$, and for the run B1 with small forcing wavelength, $k/q=5$, respectively. In both runs the forcing amplitude is small, $\tilde{\delta}=0.1+0.1i$, and the group velocity is zero, $V=0$. In agreement with analytical solutions (13), the patterns in Figs. 2 and 3 consist of traveling waves with different dispersive properties, and the magnitude of the wave $|A|$ is modulated in space and is homogeneous in time. The slope of the lines $\text{Re}(A)$ changes its sign at some locations, which correspond to sources and sinks of waves. In the domains between the sources and sinks the local amplitude and the local wave vector change the phase, Fig. 2, in accordance to the results obtained in Sec. III. In each point, the frequency $d \arg(A)/dT$ is the same, and the local phase velocity of the traveling wave, proportional to the slope of the line $\text{Re}(A)=\text{const}$, depends only on the coordinate Y and does not depend on time T . It is remarkable that the spatial domains are characterized

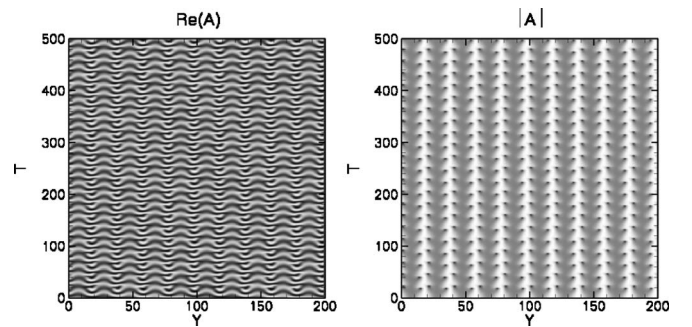


FIG. 5. Run B2, forcing with small wavelength, large amplitude, and zero group velocity.

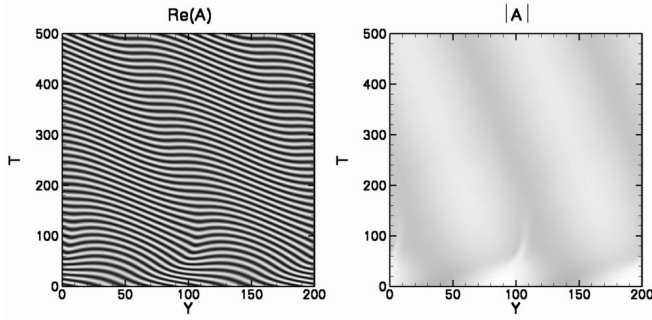


FIG. 6. Run C1, forcing with large wavelength, small amplitude, and nonzero group velocity.

by alternating signs of the phase velocity even though the modulation amplitude is rather small, see Figs. 2 and 3.

For runs A2 and B2 the forcing amplitude is large, $\delta=0.2+0.2i$, and the nonlinearity is more pronounced compared to the cases A1 and B1. Patterns in Figs. 4 and 5 are dominated by traveling waves, similar to those in Figs. 2 and 3. We see that the finite amplitude of the forcing results in appearance of high-frequency temporal components in the solutions A2 and B2, in agreement with the solutions in the Sec. III, Eqs. (5) and (6). For large-scale modulation, the pattern consists of two kinds of domains: main-frequency domains around wave “sinks,” which are characterized by a relatively small local wave vectors, and double-frequency, short-wave domains around the wave “sources,” see Fig. 4. These domains are separated by a “grain boundary,” where the phase slips are periodic (the black points in the field of $|A|$). For a short-wave modulation, the phase slips are observed as well, see Fig. 5.

For the sake of simplicity, our analytical solutions did not account for the effect of the group velocity V and the time dependence of the parametric forcing on the pattern formation. Our numerical solutions confirm the validity of this assumption. Figures 6–9 show that the solutions in the cases C1(2) and D1(2) with nonzero group velocity $V=0.01$ are similar to the cases A1(2) and B1(2) with $V=0$, respectively. We see that accounting for the group velocity V in the runs Cs and Ds induce temporal modulations of the magnitude $|A|$ and causes additional complexity. However it does not lead to nontrivial features of the nonequilibrium dynamics.

In the next series of runs, we study the influence of parametric forcing on the development of an intermittent chaos.

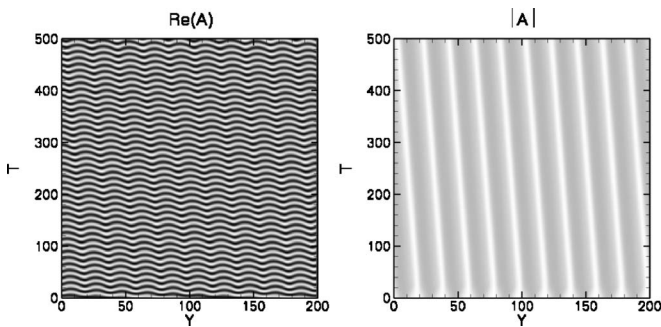


FIG. 7. Run D1, forcing with small wavelength, small amplitude, and nonzero group velocity.

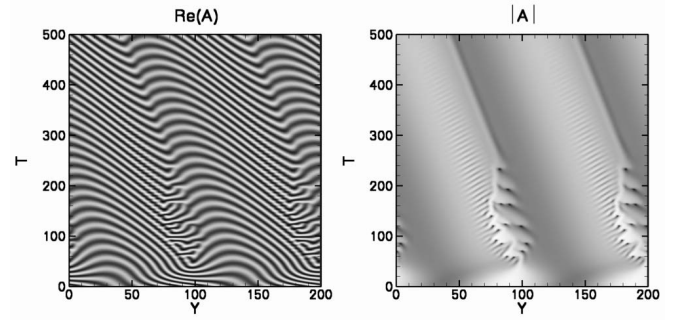


FIG. 8. Run C2, forcing with large wavelength, large amplitude, and nonzero group velocity.

According to Ref. [40,41], for unforced CGLE with $\delta=0$ in Eq. (22), the region of parameters with $c_1 > 1/2$ and $c_2 > 1$ is characterized by spatiotemporal intermittency and has chaotic solutions. To explore the forcing effect on the chaos development, we set $c_1=0.6$ and $c_2=1.4$, similarly to [40], and compute the solution for Eq. (22) for various values of the forcing parameters, see Table II.

Figure 10 shows the unforced solution for runs E0 and F0 and the development of chaos through intermittency: A wave pattern, regular initially, becomes chaotic at a finite time, identically to that in the observation of Ref. [40]. Our simulations indicate that the development of chaos is sensitive to the initial conditions. For smaller values of the wave vector of the initial perturbation q , the chaos develop for a longer time. For instance, in the case of $q=6$ the characteristic time of the chaos development is about 100 times larger than in the case of $q=10$. This sensitivity is due to the fact that without forcing the transition to chaos is triggered by the numerical errors. For smaller values of the wave vector of the initial perturbation q , the “regular wave” solution is calculated with much higher accuracy, and the errors are accumulated much slower. Our simulations indicate as well that the development of chaos may have either a transient or a “quasiperiodic” character, and the chaos generation may be sensitive to the method of the numerical solution. Figure 10 shows, for instance, that the intermittent chaos disappears at a larger time and a different regular wave pattern appear. In our simulations, the computation time is much longer than in the simulations of Ref. [40]. A more detailed quantitative comparison is hard to perform as the work [40] does not describe the numerical scheme in detail.

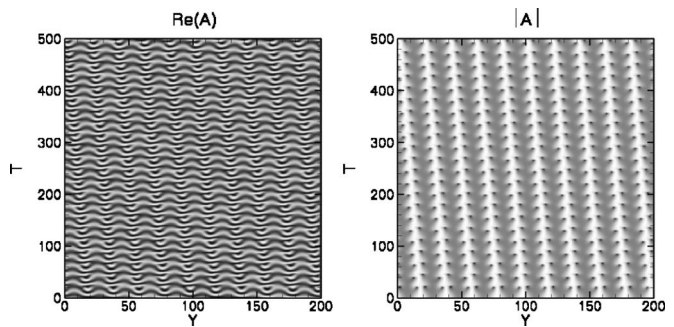


FIG. 9. Run D2, forcing with small wavelength, large amplitude, and nonzero group velocity.

TABLE II. Values of the parameters for chaotic runs.

Run	$(qL)/(2\pi)$	f	$(kL)/(2\pi)$	V
E0	10	0	0	0
E1	10	$0.05+0.05i$	2	0
E2	10	$0.05+0.05i$	2	0.01
E3	10	$0.1+0.1i$	2	0
E4	10	$0.1+0.1i$	2	0.01
F0	10	0	30	0
F1	10	$0.05+0.05i$	30	0
F2	10	$0.05+0.05i$	30	0.01
F2	10	$0.1+0.1i$	30	0
F4	10	$0.1+0.1i$	30	0.01

Accounting for the parametric forcing influences the formation of chaos dramatically. Figures 11–14 represent the numerical solutions for chaotic runs E1–E4, when the forcing has a large wavelength, $k/q=1/5$, either small or large amplitude $\tilde{\delta}$, with and without group velocity. The values of parameters q , k , V , and $\tilde{\delta}$ in runs E1–E4 correspond to those in nonchaotic runs As and Cs. Figure 11 shows the numerical solution for run E1, when the forcing amplitude is small, $\tilde{\delta}=0.05+0.05i$. We see that in this case the chaos starts to develop and then it is completely suppressed. Asymptotically, the pattern consist of traveling waves, whose magnitude $|A|$ is modulated in space and is homogeneous in time. In the run E3 the forcing amplitude $\tilde{\delta}$ is large, leading to additional complexity, see Fig. 13. However, in this case the regular regions of the solutions are easy to identify as well. Figures 12 and 14 present the solutions for the runs E2 and E4 with nonzero group velocity, $V=0.01$. We see that accounting for the group velocity, $V \neq 0$, does not change the characteristic features of the pattern and does not cause additional instabilities. Compared to the “unforced” case E0, in runs E1–E4 with large-scale forcing, the intermittent chaos develops and then disappears much faster.

For runs Fs, the forcing has small wavelength, $k/q=3$, either large or small amplitude $\tilde{\delta}$, with and without group velocity V , see Table II and Figs. 15–18. In runs Fs we choose the same wavelength of the initial perturbation as in runs Es, as for smaller values of q it takes longer for the chaos to develop. Figures 15 and 16 shows the numerical

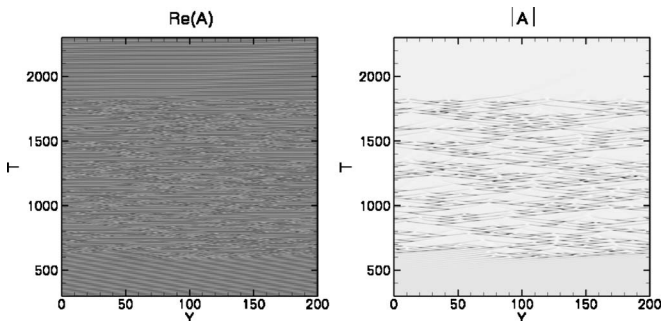


FIG. 10. Runs E0 and F0, chaotic CGLE, no forcing.

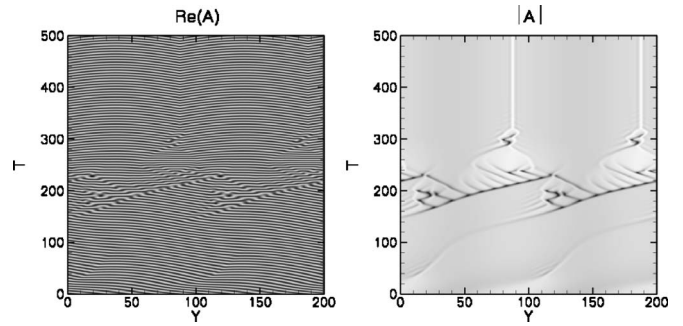


FIG. 11. Run E1, chaotic CGLE, forcing with large wavelength, small amplitude, and zero group velocity.

solution for runs F1 and F2, when the forcing amplitude is small, $\tilde{\delta}=0.05+0.05i$. Similarly to runs E1 and E2, the intermittent chaos starts to develop and then it is suppressed. The chaos suppression is complete when the forcing amplitude is large, see Figs. 17 and 18. In these cases the wave pattern remains regular for the entire computational time and the intermittent chaos does not appear.

To summarize, according to our numerical results, under parametric forcing, regular wave patterns in system (22) consist of traveling waves, whose amplitude is modulated in space and time, Figs. 2–9. The spatial modulations of the waves occurs for any value of the forcing amplitude and wavelength, whereas the high-frequency temporal components appear when the forcing amplitude is sufficiently large. The accounting for the group velocity results in additional complexity, but does cause nontrivial features of the nonequilibrium dynamics. Our simulations indicate that the intermittent chaos may be sensitive to the initial conditions and the chaotic solution may have a transient (or “quasiperiodic”) character. The parametric forcing plays a crucial role in the chaos development and may completely suppress the development of chaos.

V. DISCUSSION

We have studied the influence of heterogeneities on the nonequilibrium dynamics of wave patterns. The model is represented by the complex Ginzburg-Landau equation with parametric forcing dependent on the coordinate and time. The case of periodic nonresonant forcing has been consid-

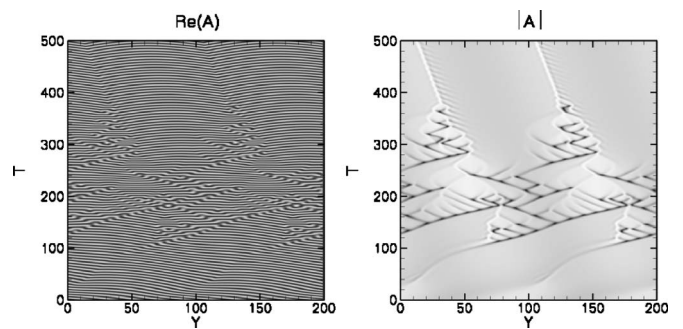


FIG. 12. Run E2, chaotic CGLE, forcing with large wavelength, small amplitude, and nonzero group velocity.

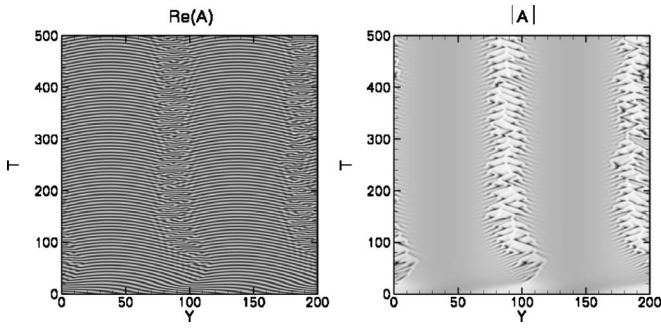


FIG. 13. Run E3, chaotic CGLE, forcing with large wavelength, large amplitude, and zero group velocity.

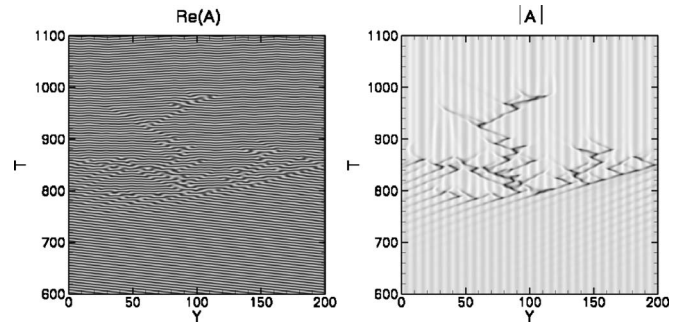


FIG. 15. Run F1, chaotic CGLE, forcing with small wavelength, small amplitude, and zero group velocity.

ered. Analytical and numerical solutions for the equation have been obtained in a wide range of the system parameters. The analysis and numerics agree with each other and indicate the new features of the nonequilibrium dynamics. We have found that in the nonchaotic case the parametric forcing results in the appearance of traveling waves with dispersion properties. For finite values of the forcing wavelength, the patterns consist of traveling waves quasiperiodic in space and (when the forcing amplitude is large enough) in time. For the forcing with very large wavelength, the nonlinear solutions have essentially anharmonic spatial structure. We have considered the influence of modulations on the development of spatiotemporal chaos. According to our results, the intermittent chaos may have a transient or quasiperiodic character, and its appearance is sensitive to the initial conditions. The parametric forcing may completely suppress the development of chaotic patterns. Accounting for the temporal dependence of the parametric forcing does not change significantly the character of the solutions obtained, in both chaotic and nonchaotic cases. The results obtained indicate a potential richness of the model, whose detailed qualitative analysis is a subject of the further research.

Our model can be applied to study the effect of surface topography on the dynamics of thermal Rossby waves. The analytical and numerical solutions in the foregoing agree with observations [37–39], which reported that qualitatively the modulations of the boundaries of the fluid tank or computational domain result in appearance of traveling waves, quasiperiodic in space and time. Compared to earlier studies

[37–39] our model (2) describes the effect of modulations on the dynamics of Rossby waves in a much wider range of the forcing parameters and convection intensity and reveals effects. These are, for instance, essentially anharmonic spatial structure of wave patterns in the case of modulations with very large wavelength and a dependence of the temporal structure of the wave patterns on the forcing amplitude. Our theory and numerics can be applied for a systematic quantitative analysis of the dispersion properties of Rossby waves influenced by the surface topography. It is worth mentioning however that our model and the results obtained have a wide range of applicability, going far beyond the Rossby waves. This includes the control of the pulse propagation in optical fibers, optical patterns, laminar-turbulent transition in a boundary layer, various instabilities in convection, and many others [1,2]. A consideration of the nonequilibrium dynamics for these phenomena are subjects of further research. The harmonic analysis, the long-term expansion, and the numerical simulations discussed in the foregoing can be used in the future studies of the influence of heterogeneities on the nonequilibrium dynamics of wave patterns.

A grip on the intermittent chaos in the systems described by CGLE is a long-standing problem, see, e.g., Refs. [43–51]. Our simulations indicate that development of chaos is a very sensible process, and a relatively weak parameter modulation is sufficient to terminate the development of chaos and to create regular wave patterns. The present work does not consider the mechanism of this phenomenon quantitatively. Qualitatively, one may expect that the parameter

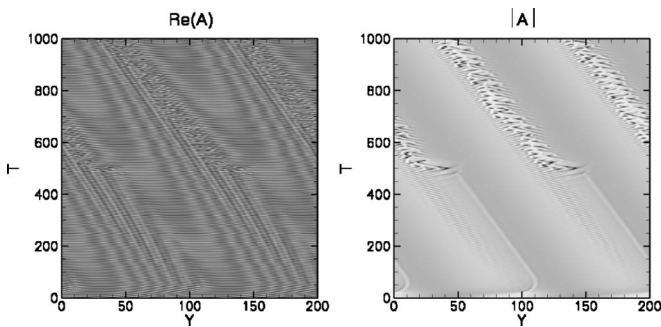


FIG. 14. Run E4, chaotic CGLE, forcing with large wavelength, large amplitude, and nonzero group velocity.

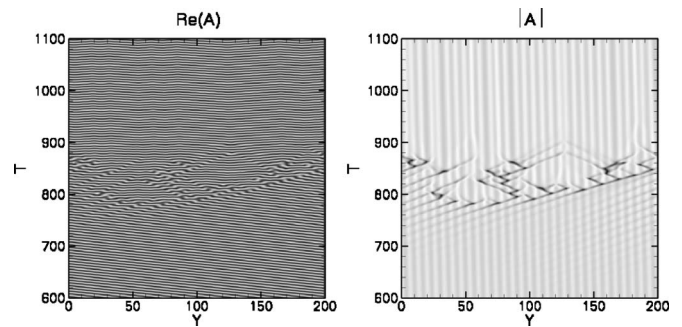


FIG. 16. Run F2, chaotic CGLE, forcing with small wavelength, small amplitude, and nonzero group velocity.

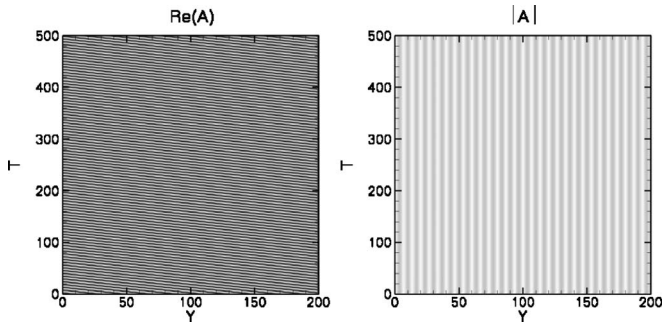


FIG. 17. Run F3, chaotic CGLE, forcing with small wavelength, large amplitude, and zero group velocity.

modulation enforces some of the Fourier amplitudes and help them to “win” in the mode competition. Without forcing, for long-wave dynamics the evolution of phase disturbances in CGLE is governed in general by one of the following nonlinear equations: Burgers equation (i), dissipation-modified Korteweg–de Vries equation (ii), and Kuramoto-Sivashinsky equation (iii). Our analytical solutions indicate that one of the effects of the parametric forcing can be a spatially distributed nonlinear phase shift. In the Eckhaus-

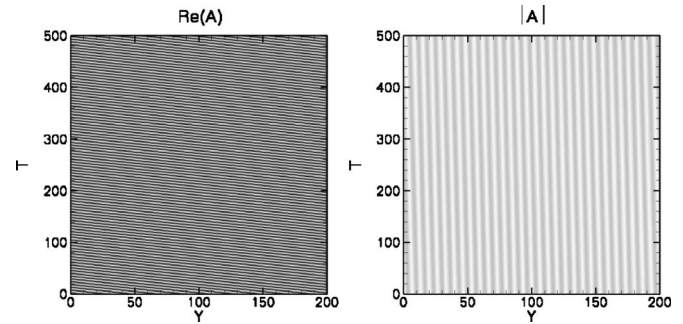


FIG. 18. Run F4, chaotic CGLE, forcing with small wavelength, large amplitude, and nonzero group velocity.

stable region, when the phase dynamics is governed by the forced Burgers equation (i), the problem can be solved using the Hopf-Cole transformation. The exploration of the Eckhaus-unstable region in the framework of models (ii) and (iii) with additional forcing term can give one a clue on how to effectively grip on the chaos development. We address these important issues in the future.

-
- [1] M. C. Cross and P. C. Hohenberg, *Rev. Mod. Phys.* **65**, 851 (1993).
- [2] I. S. Aranson and L. Kramer, *Rev. Mod. Phys.* **74**, 99 (2002).
- [3] Y. Kuramoto and T. Tsuzuki, *Prog. Theor. Phys.* **55**, 356 (1976).
- [4] K. Stewartson and J. T. Stuart, *J. Fluid Mech.* **48**, 529 (1971).
- [5] A. C. Newell, *Lect. Appl. Math.* **15**, 157 (1974).
- [6] J. T. Stuart and R. C. Di Prima, *Proc. R. Soc. London, Ser. A* **362**, 27 (1978).
- [7] Y. Pomeau, *Physica D* **23**, 3 (1986).
- [8] F. H. Busse and A. C. Or, *J. Fluid Mech.* **166**, 173 (1986).
- [9] L. P. Vozovoi and A. A. Nepomnyashchy, *J. Appl. Math. Mech.* **43**, 1080 (1979).
- [10] P. Couillet, *Phys. Rev. Lett.* **56**, 724 (1986).
- [11] E. D. Siggia and A. Zippelius, *Phys. Rev. Lett.* **47**, 835 (1981).
- [12] M. I. Tribelsky and M. G. Velarde, *Phys. Rev. E* **54**, 4973 (1996).
- [13] P. C. Matthews and S. M. Cox, *Nonlinearity* **13**, 1293 (2000).
- [14] J. Roder, H. Roder, and L. Kramer, *Phys. Rev. E* **55**, 7068 (1997).
- [15] S. J. VanHook, M. F. Schatz, W. D. McCormick, J. B. Swift, and H. L. Swinney, *Phys. Rev. Lett.* **75**, 4397 (1995).
- [16] M. M. Wu and C. D. Andereck, *Phys. Rev. Lett.* **65**, 591 (1990).
- [17] G. V. Levina and A. A. Nepomnyashchy, *Z. Angew. Math. Mech.* **66**, 241 (1986).
- [18] A. A. Nepomnyashchy, *J. Appl. Math. Mech.* **52**, 677 (1988).
- [19] C. Elphick, G. Iooss, and E. Tirapegui, *Phys. Lett. A* **120**, 459 (1987).
- [20] H. Chaté, A. Pikovsky, and O. Rudzick, *Physica D* **131**, 17 (1999).
- [21] S. Rüdiger, D. G. Míguez, A. P. Muñozuri, F. Sagues, and J. Casademunt, *Phys. Rev. Lett.* **90**, 128301 (2003).
- [22] T. Ohta and H. Tokuda, *Phys. Rev. E* **72**, 046216 (2005).
- [23] D. G. Míguez, E. M. Nicola, A. P. Muñozuri, J. Casademunt, F. Sagues, and L. Kramer, *Phys. Rev. Lett.* **93**, 048303 (2004).
- [24] J. Kim, J. Lee, and B. Kahng, *Physica A* **315**, 330 (2002).
- [25] Ch. Hemming and R. Kapral, *Physica D* **168-169**, 10 (2002).
- [26] J. Kim and J. Lee, *Phys. Rev. E* **70**, 016213 (2004).
- [27] A. Yochelis, Ch. Elphick, A. Hagberg, and E. Meron, *Physica D* **199**, 201 (2004).
- [28] B. A. Malomed, *Phys. Rev. E* **47**, R2257 (1993).
- [29] B. A. Malomed, *Phys. Rev. E* **50**, 4249 (1994).
- [30] W. Zimmermann, M. Seesselberg, and F. Petruccione, *Phys. Rev. E* **48**, 2699 (1993).
- [31] M. van Hecke and B. A. Malomed, *Physica D* **101**, 131 (1997).
- [32] C. Utzny, W. Zimmermann, and M. Bär, *Europhys. Lett.* **57**, 113 (2002).
- [33] M. Hammele and W. Zimmermann, *Phys. Rev. E* **73**, 066211 (2006).
- [34] R. Hide, *J. Fluid Mech.* **49**, 745 (1971).
- [35] K. D. Aldridge *et al.*, *Surv. Geophys.* **11**, 329 (1990).
- [36] K. K. Zhang *et al.*, *J. Fluid Mech.* **437**, 103 (2001).
- [37] P. I. Bell and A. M. Soward, *J. Fluid Mech.* **313**, 147 (1996).
- [38] J. Herrmann and F. H. Busse, *Phys. Fluids* **10**, 1611 (1998).
- [39] M. Westerburg and F. H. Busse, *Nonlinear Processes Geophys.* **10**, 275 (2003).
- [40] M. van Hecke, *Phys. Rev. Lett.* **80**, 1896 (1998).
- [41] K. Nozaki and N. Bekki, *J. Phys. Soc. Jpn.* **53**, 1581 (1984).
- [42] A. C. Or and J. Herrmann, *Phys. Fluids* **7**, 315 (1995).
- [43] D. Battogtokh and A. Mikhailov, *Physica D* **90**, 84 (1996).
- [44] D. Battogtokh, A. Preusser, and A. Mikhailov, *Physica D* **106**, 327 (1997).

- [45] K. A. Montgomery and M. Silber, *Nonlinearity* **17**, 2225 (2004).
- [46] B. Jانياud, A. Pimir, D. Bensimon, V. Croquette, H. Richter, and L. Kramer, *Physica D* **55**, 269 (1992).
- [47] W. J. Kuang and J. Bloxham, *J. Comput. Phys.* **153**, 51 (1999).
- [48] P. Coullet, J. Lega, B. Houchmanzadeh, and J. Lejzerowicz, *Phys. Rev. Lett.* **65**, 1352 (1990).
- [49] C. J. Hemming and R. Kapral, *Chaos* **10**, 720 (2000).
- [50] C. W. Meyer, G. Ahlers, and D. S. Cannell, *Phys. Rev. Lett.* **59**, 1577 (1987).
- [51] P. Coullet and K. Emilsson, *Physica A* **188**, 190 (1992).